RSC Advances

ROYAL SOCIETY OF CHEMISTRY

www.rsc.org/advances

Liquid phase oxidation of glycerol in batch and flow-type reactors with oxygen over Au-Pd nanoparticles stabilized in anion-exchange resin

Naoki Mimura* [1]

Norihito Hiyoshi [1]

Tadahiro Fujitani [2]

Franck Dumeignil * [3, 4]

1 Research Center for Compact Chemical System, National Institute of Advanced Industrial Science and Technology (AIST), 4-2-1 Nigatake, Miyagino-ku, Sendai, Miyagi, 983-8551, Japan

2 Research Institute for Innovation in Sustainable Chemistry, National Institute of Advanced Industrial Science and Technology (AIST), 16-1 Onogawa, Tsukuba, Ibaraki, 305-8569, Japan

3 Unité de Catalyse et Chimie du Solide, UCCS, UMR CNRS 8181, Université Lille 1 Sciences et Technologies, F-59655 Villeneuve d'Ascq, France.

4 Institut Universitaire de France, Maison des Universités, 106 Boulevard Saint-Michel, 75005 Paris, France.

* E-mail: n.mimura@aist.go.jp; franck.dumeignil@univ-lille1.fr

Abstract

Structure-controlled well-dispersed Au-Pd nanoparticles were successfully stabilized in a commercial ion-exchange resin. The so-obtained Au-Pd nanoparticles were tested in the liquid phase glycerol partial oxidation in the presence of molecular oxygen. They exhibited better catalytic performances than homologous monometallic Au or Pd catalysts. The optimized bimetallic catalyst trapped in the matrix of the ion-exchange resin was very stable with time on stream (> 4000 min) using a fix bed flow type reactor, with a conversion of *ca.* 50% and stable selectivities to glyceric and tartronic acids, of *ca.* 60% and 30%, respectively. The active phase originated from the presence of nanometric bimetallic nanoparticles (1.0~3.0 nm) characterized by STEM analysis.

Introduction

In the recent years, backed up by governmental incentives, the production of bio-diesel fuel (BDF) has rapidly increased. BDF is produced from vegetable oils or waste cooking oil by transesterification with methanol, conventionally using strong base catalysts such as potassium hydroxide. In this process, glycerol is formed as a by-product, which accounts for about 10 wt.% of the total product. Then, valorisation of glycerol has driven much attention for increasing the efficiency of the use of biomass resources,[1,2] either in the gas phase,[3] or in the liquid phase.[4] Within this frame, selective catalytic oxidation of glycerol to carboxylic acids in the liquid phase with oxygen as an oxidant is one of the promising routes that are explored for efficient glycerol conversion to high value added chemicals.

For the aforementioned reaction, platinum-based catalysts (Pt-Bi) were first studied by Kimura and coworkers in batch and fix bed reactors, as a pioneering work.[5] Later, gold-based catalysts, which were already well-known as efficient catalysts for low temperature oxidation of carbon monoxide[6] and for selective oxidation (epoxidation) of propylene to propylene oxide (PO),[7] have been reported. Hutchings *et al.* especially showed that carbon and TiO_2 are adequate supports for monometallic and bimetallic noble metal nano-particles (Au, Pt and Pd) used in glycerol oxidation.[8]

We focused on the preparation and the application of supported bimetallic catalysts based on gold-containing bimetallic nanoparticles, and especially on the combination of Au and Pd. For designing such systems, two types of preparation techniques can be considered. The first type consists on the formation of nanoparticles precursors on the surface of the support before obtaining

the final supported metallic nanoparticles by calcination and/or reduction treatment. In that case, the impregnation method is the typical way of preparation,[9] which is easy to operate, but which also makes it difficult to get the desired fine nanoparticles. The second type of preparation is based on nanoparticles first stabilized in the liquid phase with, *e.g.*, polyvinylpyrrolidone (PVP) or polyvinyl alcohol (PVA), before subsequent impregnation on a support. In that case, the sol-immobilization method is a typical preparation procedure[10]. After successfully designing, in the liquid phase, nanoparticles of the desired size and morphology, these features are easily kept upon impregnation. Hutchings *et al*. studied the effect of the preparation method.[11] They compared the catalytic performances of Au-Pd nanocrystals deposited on carbon supports prepared by impregnation and sol-immobilization in the reactions of benzyl alcohol oxidation and H_2O_2 formation. The higher activity of the sol-immobilised catalysts was ascribed to the formation Au–Pd nano-alloy particles with a narrower size range.

Au-Pd bimetallic nanoparticles are also very efficient catalysts for glycerol oxidation. For this purpose, they were prepared by sol-immobilized (or sol-immobilization like) method and supported on carbon-based materials;[12] Davis *et al.* reported active carbon-supported Au-Pd catalysts prepared by deposition-reduction and sol-immobilization methods;[13] Hutchings *et al.* reported Au-Pd catalysts also prepared by both the impregnation and the sol-immobilization methods on carbon, TiO_2 and Fe_2O_3 supports.[8(c)] The activities of the catalysts prepared by the sol-immobilization method generally exhibited higher activities in glycerol oxidation than that of the catalysts prepared by the impregnation method. Hutchings *et al.* also reported AuPt and AuPd

catalysts supported on MgO, with the advantage of getting rid of the use of a basic medium to enable glycerol oxidation reaction.[14]

After the use of inorganic supports polymers have then driven much attention as effective ways of supporting/stabilizing nanoparticles, while avoiding the aforementioned drawbacks. Ishida and Haruta *et al.* have developed several types of catalysts based on gold on resin for oxidation and reduction reactions.[15] Further, Kobayashi *et al.* reported that gold nanoclusters stabilized by the benzene rings of polystyrene derivatives are efficient catalysts for the oxidation of alcohols at room temperature.[16] Furthermore, Mori and Yamashita *et al.* prepared nano-sized Pd particles in cation-exchange resin exhibiting a strong acidity, which gave a catalytic system efficient for hydrogen peroxide production from $H_2 + O_2$.[17] Villa *et al.* reported gold nanoparticles stabilized by using tetrakishydroxypropylphosphonium chloride (THPC) on anionic-exchange resin (Dowex M-43) as a catalyst for glycerol oxidation in both batch-type reactor and fixed bed flow type reactor.[18] The advantage of such a method was to yield 5.43 nm gold nanoparticles (average diameter) instead of 8.78 nm in the case of the direct, THPC-free, ion-exchange method. The THPC-stabilized Au/resin catalyst performances were stable with time on stream (22 h), with, however, at 323 K, a rather modest glycerol conversion of *ca.* 20~25% and selectivities to glyceric and tartronic acids of *ca.* 40% and 20%, respectively. There are only a few research reports about Au-Pd nanoparticles fixed in ion-exchange resins, despite the expected merits compared to monometallic formulations. For exploiting the aforementioned synergistic effect of Au-Pd bimetallic active species, the Au-Pd/resin system is promising as a catalyst for glycerol oxidation.

In the present paper, we present the catalytic activity of Au-Pd nanoparticles (of which the distribution homogeneity was checked by the EDS technique) immobilized in an anion-exchanged resin for the liquid phase oxidation of glycerol using molecular oxygen as an oxidant. Moreover, we also present here the relationship between catalytic activities, preparation methods and structure (morphology) of the nanoparticles fixed in an anion-exchange resin. The merits of the proposed method lies in the fact that *(i)* the preparation technique of such nanoparticles catalyst is very easy and *(ii)* the observed activities and selectivities are high and stable in a long-term continuous operation (fixed bed flow type reactor).

Experimental

The precursors of Au and Pd were $HAuCl_4$ (Wako Pure Chemical Industries, Ltd., Tokyo, Japan) and $PdCl_2$ (Wako), respectively. Because palladium chloride is not easy to dissolve in water, a small amount of choric acid solution was used as a first solvent for $PdCl_2$. Then, 100 mL of water and $HAuCl_4$ were added to the Pd solution to prepare an Au-Pd mixed solution. A desired amount of anion-exchange resin (Amberlite IRA402BLCL, Organo, Tokyo, Japan) was subsequently added to the Au and Pd mixed solution. Then, this solution was stirred using a magnetic stirrer for 20 min at room temperature. The colour of the solution changed from yellow-orange to colourless, which enabled confirming at a glance that all the Au and Pd anions were exchanged with the Cl^- of the resin. $NaBH_4$ for reduction was then added to the solution, and the colour of the catalyst changed from yellow-orange to black or brown. After washing the resin including reduced Au and Pd

particles, it was further treated with a NaOH solution to exchange the remaining Cl^- ions with OH^- ions. At last, the so-obtained catalytic resin was washed using ion-exchanged water before being dried at 313 K in air.

Catalysts preliminary screening experiments were performed in a stainless steel batch-type reactor (inner diameter = 50 mm, depth = 170 mm, volume = 300 mL, Taiatsu Techno, Tokyo, Japan). The glycerol solution (100 mL, 0.3 mol/L) was placed in the hermetically closed reactor with NaOH (Wako, 4.8 g, *i.e.*, NaOH/GLY = 4 in the case of standard test conditions) and 0.5 g of catalyst. The initial pressure of molecular oxygen was adjusted at 1.0 MPa at room temperature. The oxidation reaction was started by soaking the reactor in a water bath regulated at 333 K, and stopped by quenching in an ice bath at 273 K.

The oxidation of glycerol runs in a flow type reactor were operated in a duplex glass tube (Model GJ-08, Sibata Scientific Technology Ltd., Saitama, Japan, inner diameter = 8.0 mm, length = 300 mm). An outline of the flow reactor system is shown in Figure 1. The weight and volume of catalyst were 5.0 g and 8.3 mL, respectively, and the detailed reaction parameters are as follows: The reaction temperature was controlled at 333 K by using a hot water pump, which circulated water in the outer jacket of the duplex glass tube. The oxygen pressure at the inlet of the reactor was set at 0.5 MPa. The oxygen line was controlled by mass-flow controller (Honma Riken, Saitama, Japan) and the liquid line (glycerol concentration = 0.3 mol/L, molar ratio of NaOH/glycerol = 4) was fed using a plunger pump (Model NP-DX, Nihon Seimitsu Kagaku, Co. Ltd., Tokyo, Japan). Both lines were connected by a T-connector (Swagelok, Ohio, USA). The

outlet of the reactor was opened to the atmosphere, and the solution was periodically sampled in Erlenmeyer flasks.

The reaction products were analysed by a high-pressure liquid chromatography (HPLC, Shimadzu, Kyoto, Japan) equipped with a column designed for the analysis of sugars and organic acids (ICSep-Coregel 107H, Tokyo Kasei Co. Ltd., Tokyo, Japan) after neutralization by addition of H_2SO_4. The moving phase for HPLC was a H_2SO_4 solution (0.018 N) and the feed rate was 0.4 mL/min. This device enabled good separation of products, which were identified by comparison with commercial reagents as standard materials. There were some un-identified peaks by using commercial standard materials, unfortunately.

The catalysts were analysed by a transmission electron microscope (EM-002B, Topcon, Tokyo, Japan) and an analytical electron microscope equipped with a high-resolution energy dispersive X-ray spectrometer (JEM-ARM200F, JEOL, Tokyo, Japan).

Results and discussion

Figure 2 shows conversions and selectivities to glyceric and tartronic acids (GLYA and TA, respectively) in glycerol oxidation over Au-Pd bimetallic catalysts as a function of the Au / (Au +Pd) molar ratio. The catalyst with an equivalent number of Au and Pd atoms exhibited the best catalytic performance in terms of GLYA+TA yield (*ca.* 76%, with a conversion of 88.5% and a summed selectivity of 85.8%). The other identified minor products were glycolic acid (selectivity: *ca.* 7.5%), oxalic acid (selectivity: *ca.* 1.7%) and lactic acid (selectivity: *ca.* 2.4%),

which were formed by overoxidation and C-C bond cleavage of C_3 products. The same trend for the distribution of by-products was observed on the studied series of catalysts.

For the Au-Pd bimetallic systems prepared by the sol-immobilization method, Hutchings *et al.* prepared a catalyst with 1.0 wt.% of noble metals and with a Au:Pd=1:1 weight ratio, and a catalyst also containing 1.0 wt.% of noble metals but with a Au:Pd=1:1 atomic ratio[8(c)]. The TOF (turn over frequency) of the catalyst with 1:1 atomic ratio was superior to that of the catalyst with 1:1 weight ratio, when supported on carbon or TiO_2. The trend is similar in the case of the present Au-Pd/ion-exchange resin catalysts shown in Fig.2 [when the weight ratio is 1:1, the atomic percentage of Au/(Au+Pd) is about 35.2 %] On the other hand, the behaviours of Au-Pd catalysts nanoparticles deposited on a carbon support with various Au/Pd ratios reported by Davis[13] were a little bit different from those of our catalysts. The main difference was the observation of a higher TOF over the Au monometallic catalyst of Davis. However, a similar trend was observed for the selectivity to glyceric acid that increased over Au-Pd bimetallic particles (atomic ratio of Au:Pd = 0.15~0.56). The differences of the behaviours of the Au-Pd nanoparticle catalysts are considered to be caused by the differences of preparation procedures and by the interaction between the supports and the active nanoparticles.

TOF of the oxidation in the batch type reactor was calculated as follows:

TOF (h^{-1}) = [Converted glycerol molecule in the reaction time (mol/h)] / [Au+Pd catalyst metal (mol)]

The TOF of catalyst No.1 in Table 1 was 1602 h^{-1}, which is reasonable compared with previous studies. Indeed, typical TOFs of Au-Pd bimetallic catalysts prepared by a sol-immobilization method were between 500 h^{-1} (average over 4 h of reaction) and 4000 h^{-1} (initial TOF determined for the first 30 min of reaction).[8(c)]

The effect of the preparation procedure on the performances of the catalyst with the optimal molar ratio of 50% Au and 50% Pd is summarized in Table 1. The effects of the Au and Pd introduction order (simultaneous or sequential) and of the reduction step (final or sequential) were systematically studied. As a result, and considering the observed catalytic performances, the best way for preparing efficient Au-Pd catalysts was ion exchange with a Au-Pd mixed solution followed by a one shot reduction. Using well-mixed bimetallic nanoparticles then seems to be an important parameter to induce good catalytic performances.

Figure 3 shows TEM images of Au-Pd particles enclosed in the anion-exchange resin, which is catalyst No.1 listed in Table 1. It appears at a glance that the particle size is quite homogeneous with well dispersed nanoparticles, with a sphere-like shape. Figure 4 further shows STEM-HAADF images of the catalyst No.1 and particle size distribution of the catalyst determined using STEM-HAADF images. 90% of the particles have a diameter in the range from 1.0 nm to 3.0 nm. Especially, 50% of particles are in the range from 1 nm to 2 nm. Figure 5 shows the results of high-resolution EDS analysis of a typical nanoparticle observed in catalyst No.1. The EDS images indicate that gold and palladium are at almost the same location in the matrix of ion-exchange resin. It can then be considered that Au and Pd are well-mixed like as a nano-alloy, which is related to

higher catalytic performance. The two-step preparation method (ion-exchange of (Au+Pd) mixed solution → reduction by using $NaBH_4$) is considered to be effective for obtaining well-mixed nano-particles in the resin. After the ion exchange using the Au-Pd mixed solution, the complexes of $AuCl_4^-$ and $PdCl_4^{2-}$ fixed instead of Cl^- on the anion exchange sites are supposedly arranged in a random order, with a statistic distribution. Thus, well-mixed Au-Pd bimetallic particles (shown in Figure 5) are formed from Au and Pd precursors in a random arrangement by *in situ* liquid phase reduction using $NaBH_4$.

Other preparation methods shown in entry 2 to 5, for example, were comparatively not so effective, because well-dispersed random arrangements of Au and Pd on the ion-exchange sites before reductions were not achieved due to sequential introduction of the metal precursors, and the Au and Pd atoms were thus not well-mixed after $NaBH_4$ treatments. Figure 6 shows the STEM-HAADF image and size distribution of Au-Pd nano-particle in catalyst No.2, which is prepared by a 4 steps method (Au ion-exchange → 1^{st} reduction → Pd ion-exchange →2^{nd} (last) reduction). The size distribution of the nano-particles is shifted to a larger size than that observed over catalyst No.1. Especially, the proportion of particles over 3.0 nm significantly increased (from 6.4 % on catalyst No.1 to 19.1 % on catalyst No.2). The more pronounced presence of particles with a larger size might be a reason for the observed lower catalytic performances. The structure of the nanoparticles is observed as a core-shell like structure shown in Figure 7, as observed by high-resolution EDS analysis. The core is gold and the shell is palladium. This observation can be reasonably interpreted because gold core was the 1^{st} element fixed in the matrix as reduced metallic

nanoparticles and then palladium precursor was fixed on the freed ion-exchange sites just next to the metallic gold particles. The heterogeneous structure of nanoparticles in that case, namely in the case in which Au and Pd are not well-mixed, can be accounted for a second important reason for the observed lower activity.

Figure 8 shows STEM-HAADF image and size distribution of Au-Pd nano-particle in catalyst No.3, which is also prepared by a 4 steps method (Pd ion-exchange → 1st reduction → Au ion-exchange →2nd (last) reduction). The size distribution is almost same as that observed over the above-described catalyst No.2. Further, Figure 9 suggests that Au and Pd in the particle are not well-mixed, with a three layered core-shell structure. Although the detailed mechanism of formation of such a three layer structure is not clear, the heterogeneous particle structure together with a larger particle size can also largely explain the lower catalytic performances of this sample. Similar phenomena about the structure of nanoparticles have been already reported about Au-Pd or Au-Ag nanoparticles trapped in dendrimers or organic frameworks.[19]

We will now discuss about the active species - or active sites - based on the above-mentioned catalytic reaction results and microscope analysis. The actual effective active site is considered to be an Au-Pd mixed nanoparticle surface, with a synergistic effect of the combination of Au and Pd. This synergy is optimal at an atomic percentage of Au in (Au+Pd) of 30~50%, with a high conversion together with a high selectivity, as reported in Fig. 2. For the core-shell type morphology (Catalysts No.2 and 3), the surface is covered with Pd, as suggested by the results of high-resolution EDS analysis. The catalytic activity of Pd is very low (Fig. 2). Thus, the catalytic activity of the

core-shell catalyst is not so good as well. In contrast with core-shell type catalysts, well-mixed nanoparticle (catalyst No.1) are more effective for oxidation, because the surface is considered to be well-mixed structure composed of Au and Pd. This is also in good agreement with the fact that a catalyst containing only Au in the resin was not so active (Fig.2). Addition of alkali as a promoter is very important for glycerol oxidation over Au-Pd catalys[8,12,13]. The effect of NaOH can also be assessed by comparing data in Table 1: Comparing entries No. 1, 6 and 7, the importance of the addition of NaOH is clearly demonstrated. Indeed, the catalyst is inactive in the absence of NaOH (Entry 7) and, then, conversion increases with the NaOH to glycerol molar ratio with values increasing from 53.4% to 88.5% for ratios of 1 and 4, respectively. The effects of the addition of alkali were reported by many research groups cited above. In addition, Skrzyńska *et al.* previously reported an explained the results of glycerol oxidation with NaOH in the absence of a catalyst[20] (only NaOH was added to the reactant solution). Then, comparing entry No. 1 and 8, we can also remark that NaOH is superior to KOH as an alkali promoter, with a conversion of 59.4% and 88.5%, respectively. A similar trend of the promoter effect of alkalis in the oxidation of 1,2-propanediol to lactic acid over AuPt bimetallic catalysts was reported by Hutchings *et al.*[21] They explained that the reason of a loss of activity was that the active surfaces of catalysts might be covered by the larger cations.

In our catalyst, the chemical interaction between the Au-Pd bimetallic nanoparticles and the matrix ion-exchange resin can be considered as very weak or quasi-inexistent in the aqueous medium, and the behaviour of the catalyst is most likely to be similar to that of unsupported gold

nanoparticles-based catalysts. The reaction pathways of the glycerol oxidation with and without unsupported gold catalysts in the case of addition of alkali (NaOH) as a promoter were discussed in detail by Skrzyńska *et al.*[20] Practically, the distribution of target products and by-products of Au-Pd nanoparticle fixed in ion-exchange resin can be accounted based on the reaction scheme presented in the aforementioned paper. Further, the role of palladium in the Au-Pd nanoparticles increases the conversion while hindering the C-C bond cleavage activity,[13] which produces C_2 products such as glycolic, oxalic and lactic acids.

Ion-exchange resin is very suitable for being used in a liquid phase flow type reactor, because the particles are beads-like (with a diameter comprised between 0.5 and 1.0 mm). Thus, we designed a flow reactor to verify the effectiveness and the stability of the catalysts. Figure 10 shows the results of long-term flow reaction (the detail of the reaction conditions is summarized in the caption of the figure). The catalytic activity was very stable during the tested reaction period (Figure 10). The selectivity to tartronic acid was higher than in the batch type reactor (Table 1, entry No.1 and Figure 10). We can postulate that the carboxylic acid anion is weakly trapped in the ion exchange resin and moved slower than the flow rate of water as the solvent. Thus, the actual contact time was longer. The result of long-term oxidation indicates that ion-exchange resin is very effective support for liquid phase flow reaction. Unfortunately, the TOF measured for the flow-type catalytic reaction was 34.1 h^{-1} at the steady state (from 800 min to 1800 min in Fig.10), which is relatively low compared with the batch-type reactions. This is due to two reasons. The first one is that the liquid and gas phases were not well mixed in the reactor because stirring was not performed in the flow

reactor (the stirring speed was 750 rpm in the case of the batch-type reactor). The second reason is that the pressure of oxygen was not so high (0.5 MPa at the inlet of the reactor, and the end of the reactor was open to the atmosphere). Engineering design of reactor focused on the development of a proper mixing technique and a well-controlled oxygen pressure is then worth exploring, in order to improve such kind of liquid/gas flow reaction technology, which can thus be the next research target in the field.

Conclusions

Well-dispersed and structure-controlled Au-Pd nanoparticles stabilized in the matrix of anion-exchange resin were successfully prepared by ion-exchange method. The catalytic activity of bimetallic Au-Pd catalyst was higher than that of monometallic Au or Pd catalysts. The catalytic performances were affected by the preparation procedure, which influenced the relative distribution of Au and Pd in the nanoparticle, this latter being optimal by simultaneous introduction of the metal precursors instead of a sequential way. Further, microscope analysis (STEM and high-resolution EDS) clearly shows that smaller nanoparticles in a Au and Pd well-mixed nano-alloy gave better catalytic performances.

The bimetallic catalyst was suitable for fix bed flow type reactor, shown in Figure 1, and the catalytic activity was very stable in long-term reaction (> 4000 min), shown in Figure 10.

Acknowledgements

A part of this work was supported by Japan Society for the Promotion of Science (JSPS) KAKENHI Grant Number 25340130 and by the International Research Group 'ECSAW' (Environmental Catalysis for Sustaining Clean Air and Water) between CNRS and AIST. The authors want also to thank Professor M. Shirai of Iwate University and AIST for helpful comments and advices for this research.

References

[1] M. Pagliaro, R. Ciriminna, H. Kimura, M. Rossi and C. Della Pina, *Angew. Chem. Int. Ed. Engl.*, 2007, 46, 4434-4440.
[2] M. Pagliaro, M. Rossi, in The Future of Glycerol 2nd Edition, RSC Green Chemistry Book Series, **2010**.
[3] B. Katryniok, S. Paul, F. Dumeignil, *ACS Catal.*, 2013, 3, 1819-1834.
[4] B. Katryniok, H. Kimura, E. Skrzyńska, J.-S. Girardon, P. Fongarland, M. Capron, R. Ducoulombier, N. Mimura, S. Paul and F. Dumeignil, *Green Chem.*, 2011, 13, 1960-1979.
[5] (a) H. Kimura, K. Tsuto, T. Wakisaka, Y. Kazumi and Y. Inaya, Appl. Catal. A, 1993, 96, 217-228, (b) H. Kimura, *Appl. Catal. A*, 1993, 105, 147-158.
[6] M. Haruta, S. Tsubota, T. Kobayashi, H. Kageyama, M. J. Genet and B. Delmon, *J. Catal.*, 1993, 144, 175-192.
[7] A. K. Sinha, S. Seelan, S. Tsubota and M. Haruta, *Angew. Chem. Int. Ed. Engl.*, 2004, 43, 1546-1548.
[8] (a) S. Carrettin, P. McMorn, P. Johnston, K. Griffin and G. J. Hutchings, *Chem. Commun*., 2002, 696-697, (b) S. Carrettin, P. McMorn, P. Johnston, K. Griffin, C. J. Kiely and G. J. Hutchings, *Phys. Chem. Chem. Phys.*, 2003, 5, 1329-1336, (c) N. Dimitratos, J. A. Lopez-Sanchez, J. M. Anthonykutty, G. Brett, A. F. Carley, R. C. Tiruvalam, A. A. Herzing, C. J. Kiely, D. W. Knight and G. J. Hutchings, *Phys. Chem. Chem. Phys.*, 2009, 11, 4952-4961.
[9] (a) J. K. Edwards, B. E. Solsona, P. Landon, A. F. Carley, A. Herzing, C. J. Kiely and G. J. Hutchings, J. Catal., 2005, 236, 69-79. (b) J. K. Edwards, B. Solsona, P. Landon, A. F. Carley, A. Herzing, M. Watanabe, C. J. Kiely and G. J. Hutchings, J. Mater. Chem., 2005, 15, 4595-4600. (c) D. I. Enache, J. K. Edwards, P. Landon, B. Solsona-Espriu, A. F. Carley, A. A. Herzing, M. Watanabe, C. J. Kiely, D. W. Knight and G. J. Hutchings, Science, 2006, 311, 362-365. (There are too many references to list here all.)
[10] (a) L. Kesavan, R. Tiruvalam, M. H. A. Rahim, M. I. bin Saiman, D. I. Enache, R. L. Jenkins, N. Dimitratos, J. A. Lopez-Sanchez, S. H. Taylor, D. W. Knight, C. J. Kiely and G. J. Hutchings, Science, 2011, 331, 195-199. (b) R. C. Tiruvalam, J. C. Pritchard, N. Dimitratos, J. A. Lopez-Sanchez, J. K. Edwards, A. F. Carley, G. J. Hutchings and C. J. Kiely, Faraday Discuss., 2011, 152, 63-86. (c) A. Villa, D. Wang, P. Spontoni, R. Arrigo, D. Su and L. Prati, Catal. Today, 2010, 157, 89-93. (d) A. Villa, N. Janjic, P. Spontoni, D. Wang, D. S. Su and L. Prati, Applied Catalysis A: General, 2009, 364, 221-228. (There are too many references to list here all.)
[11] J. A. Lopez-Sanchez, N. Dimitratos, P. Miedziak, E. Ntainjua, J. K. Edwards, D. Morgan, A. F. Carley, R. Tiruvalam, C. J. Kiely and G. J. Hutchings, Phys. Chem. Chem. Phys., 2008, 10, 1921-1930.
[12] (a) C. L. Bianchi, P. Canton, N. Dimitratos, F. Porta and L. Prati, Catal. Today, 2005, 102-103, 203-212. (b) N. Dimitratos, J. Lopez-Sanchez, D. Lennon, F. Porta, L. Prati and A. Villa, Catal. Lett., 2006, 108, 147-153. (c) N. Dimitratos, F. Porta and L. Prati, Applied Catalysis A: General, 2005, 291, 210-214. (d) N. Dimitratos, A. Villa and L. Prati, Catal. Lett., 2009, 133, 334-340.
[13] W. C. Ketchie, M. Murayama and R. J. Davis, J. Catal., 2007, 250, 264-273.
[14] G. L. Brett, Q. He, C. Hammond, P. J. Miedziak, N. Dimitratos, M. Sankar, A. A. Herzing, M. Conte, J. A. Lopez-Sanchez, C. J. Kiely, D. W. Knight, S. H. Taylor and G. J. Hutchings, Angew. Chem. Int. Ed., 2011, 50, 10136-10139.
[15] (a) T. Ishida, K. Kuroda, N. Kinoshita, W. Minagawa and M. Haruta, *J. Colloid Interface Sci.*, 2008, 323, 105-111, (b) T. Ishida, S. Okamoto, R. Makiyama and M. Haruta, *Appl. Catal. A*, 2009, 353, 243-248, (c) K. Kuroda, T. Ishida and M. Haruta, *J. Mol. Catal. A*, 2009, 298, 7-11, (d) T. Ishida and M. Haruta, *Angew. Chem. Int. Ed. Engl.*, 2007, 46, 7154-7156.
[16] H. Miyamura, R. Matsubara, Y. Miyazaki and S. Kobayashi, *Angew. Chem. Int. Ed. Engl.*, 2007, 46, 4151-4154.
[17] K. Mori, A. Hanafusa, M. Che and H. Yamashita, *J. Phys. Chem. Lett.*, 2010, 1, 1675-1678.
[18] A. Villa, C. E. Chan-Thaw and L. Prati, *Appl. Catal. B*, 2010, 96, 541-547.
[19] (a) R. W. J. Scott, O. M. Wilson, S.-K. Oh, E. A. Kenik and R. M. Crooks, *J. Am. Chem. Soc.*, 2004, 126, 15583-15591. (b) H.-L. Jiang, T. Akita, T. Ishida, M. Haruta and Q. Xu, *J. Am. Chem. Soc.*, 2011, 133, 1304-1306.
[20] E. Skrzyńska, J. Ftouni, J.-S. Girardon, M. Capron, L. Jalowiecki-Duhamel, J.-F. Paul and F.Dumeignil. *Chem Sus Chem*, 2012, 5, 2065-2068.
[21] Y. Ryabenkova, Q. He, P. J. Miedziak, N. F. Dummer, S. H. Taylor, A. F. Carley, D. J. Morgan, N. Dimitratos, D. J. Willock, D. Bethell, D. W. Knight, D. Chadwick, C. J. Kiely and G. J. Hutchings, *Catal. Today*, 2013, 203, 139-145.

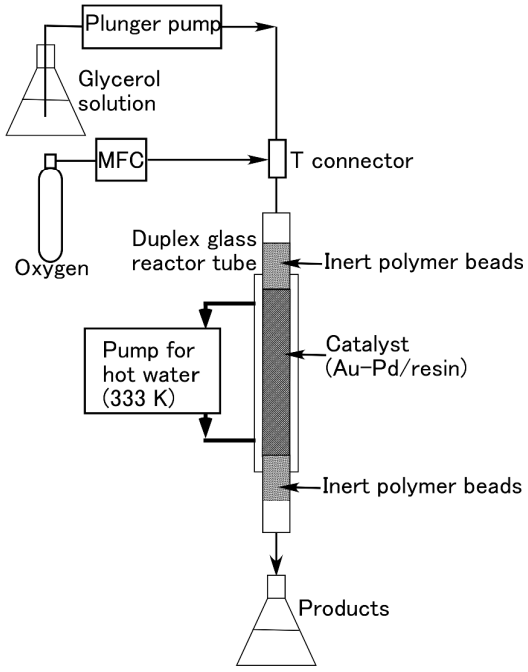

Fig. 1 Setup of fixed bed flow reactor for oxidation of glycerol.

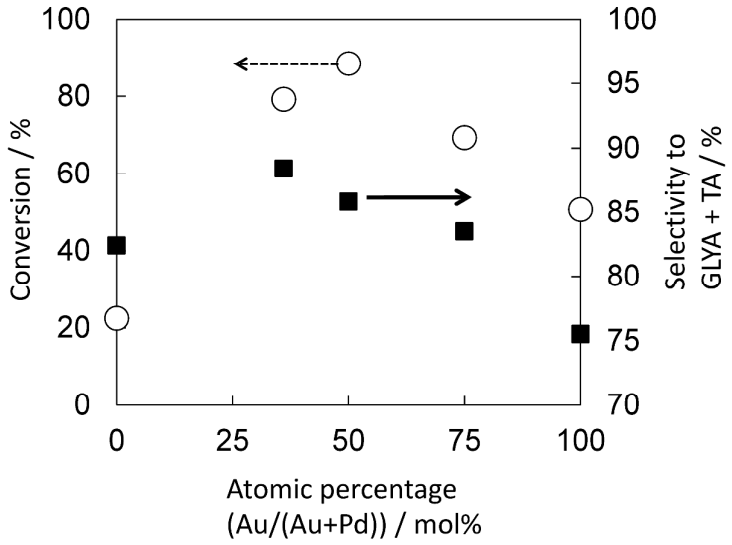

Fig. 2 Catalytic performances of Au-Pd nanoparticle catalysts with various Au atomic percentages.
○: Conversion of glycerol, ■: Summed selectivities to glyceric and tartronic acids (GLYA + TA.)
Reaction conditions:
Catalyst weight: 0.5 g (Content of (Au+Pd): 0.5 wt.%);
Glycerol concentration: 0.3 mol/L; Temperature: 333 K; Stirring speed: 750 rpm; Initial pressure of oxygen: 1.0 MPa.

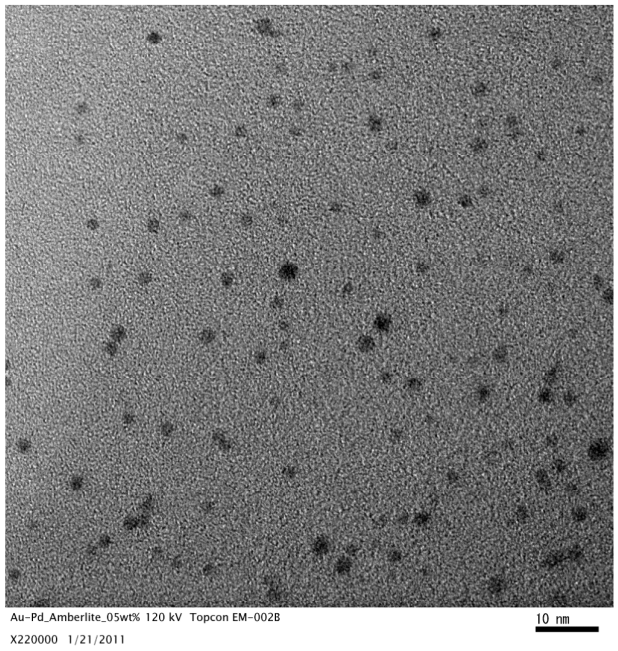

Fig. 3 TEM image of Au-Pd nanoparticles stabilized in the ion-exchange resin. (Catalyst No.1, Au+Pd = 0.5 wt.%, Au:Pd atomic ratio = 50:50.)

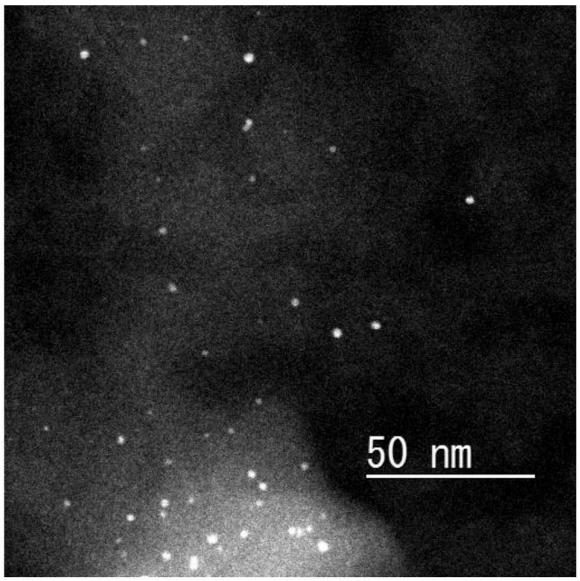

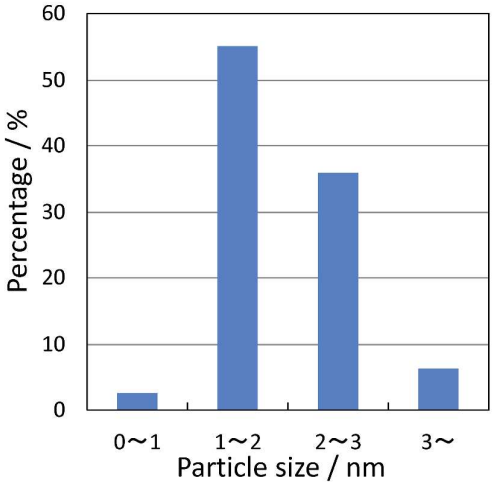

Fig. 4 STEM-HAADF image and size distribution of Au-Pd nano-particle in catalyst No.1.
(Statistics were performed on 78 particles. All STEM images for measuring size distribution are shown in Supporting information 1.)

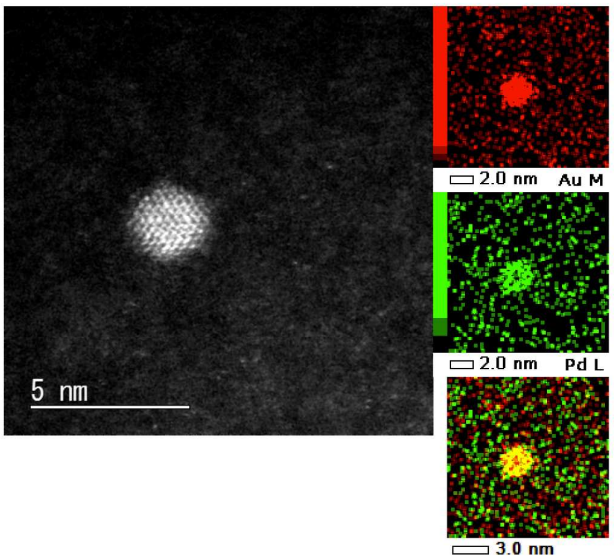

Fig. 5 STEM-HAADF image and high-resolution EDS analysis of a typical Au-Pd nanoparticle observed in Catalyst No.1.

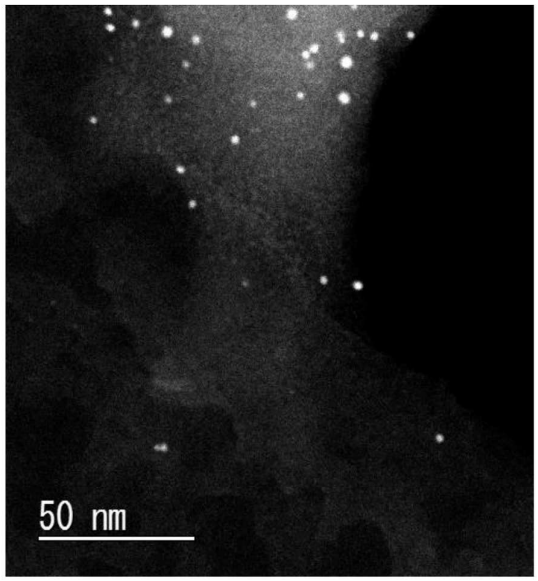

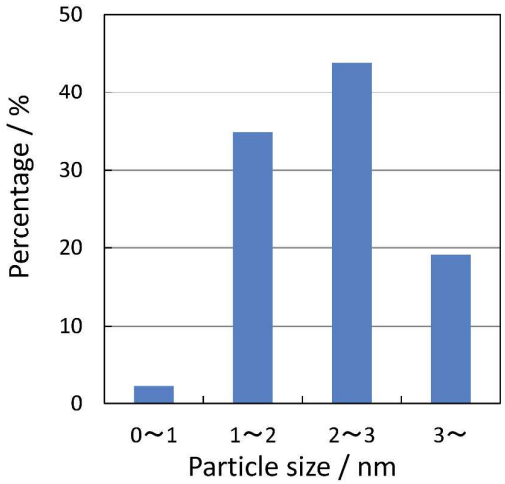

Fig. 6 STEM-HAADF image and size distribution of Au-Pd nano-particle in catalyst No.2.
(Statistics were performed on 89 particles. All STEM images for measuring size distribution are shown in Supporting information 1.)

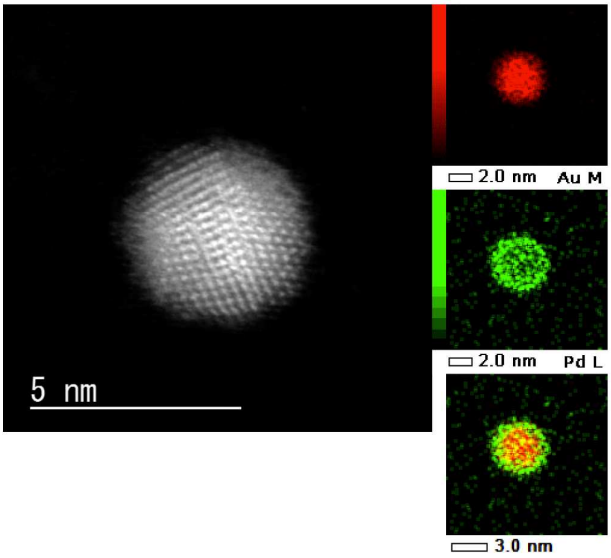

Fig. 7 STEM-HAADF image and high-resolution EDS analysis of Au-Pd nano-particle in Catalyst No.2.

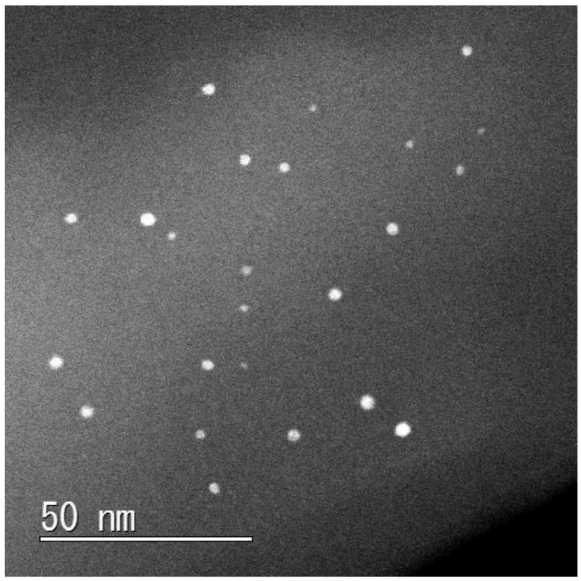

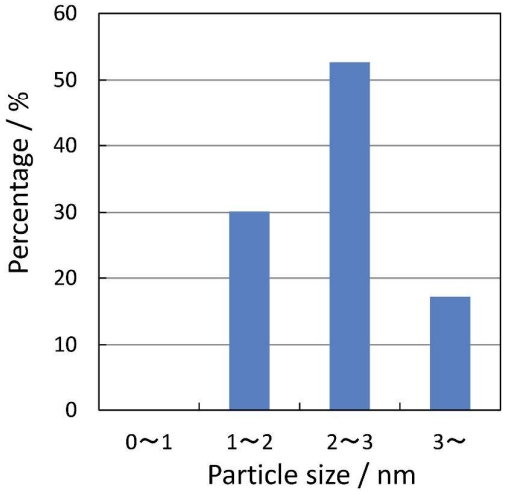

Fig. 8 STEM-HAADF image and size distribution of Au-Pd nano-particle in catalyst No.3.
(Statistics were performed on 93 particles. All STEM images for measuring size distribution are shown in Supporting information 1.)

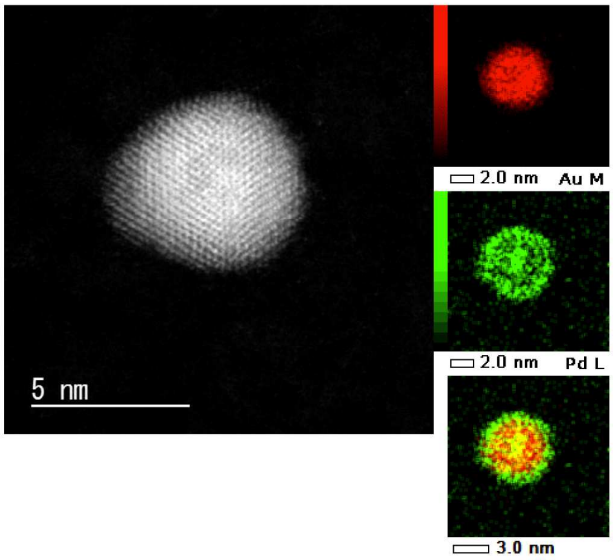

Fig. 9 STEM-HAADF image and high-resolution EDS analysis of Au-Pd nano-particle in Catalyst No.3.

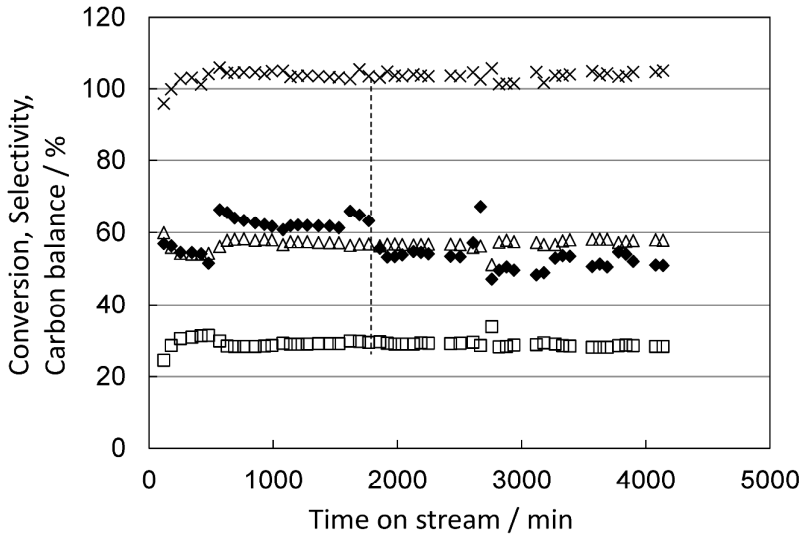

Fig. 10 Long-term catalytic reaction test of glycerol oxidation using flow type reactor.

0~1800 min: Glycerol solution liquid flow: 0.5 mL/min, Oxygen flow：3.5 mL/min
1800~4170 min: Glycerol solution liquid flow：0.6 mL/min, Oxygen flow：4.2 mL/min

Reactor: glass column for high pressure (inner diameter: 8.0 mm, length: 300 mm),
Catalyst weight: 5.0 g (volume: 8.3 mL), Reaction temperature: 333 K
Feed mixed solution liquid flow: glycerol 0.3 mol/L＋NaOH 1.2 mol/L
×: carbon balance, ◆: Conversion of glycerol, △: selectivity to glyceric acid, □: selectivity to tartronic acid.

Table 1 Effects of the preparation method and of the addition of NaOH on the catalytic performances of the Au:Pd 50:50 catalyst in the oxidation of glycerol using molecular oxygen as an oxidant.

Entry	Catalyst No.	Preparation procedure	NaOH / Glycerol / mol/mol	Conversion / %	Selectivity /%	
					Tartronic acid	Glyceric acid
1	1	(1) Au+Pd ion exchange → (2) reduction	4	88.5	9.6	76.2
2	2	(1) Au ion exchange → (2) reduction → (3) Pd ion exchange → (4) reduction	4	69.0	8.7	75.1
3	3	(1) Pd ion exchange → (2) reduction → (3) Au ion exchange → (4) reduction	4	48.9	8.8	74.8
4	4	(1) Au ion exchange → (2) Pd ion exchange →(3) reduction	4	60.1	10.9	72.9
5	5	(1) Pd ion exchange → (2) Au ion exchange → (3) reduction	4	71.3	8.1	78.0
6	1	(1) Au+Pd ion exchange → (2) reduction	1	53.4	10.0	74.8
7	1	(1) Au+Pd ion exchange → (2) reduction	0	0	-	-
8	1	(1) Au+Pd ion exchange → (2) reduction	4*	59.4	7.9	75.1

Reaction conditions:

Catalyst weight: 0.5 g (Au/Pd atomic ratio: 1, content of (Au+Pd): 0.5 wt.%);

Glycerol concentration: 0.3 mol/L;

Temperature: 333 K;

Stirring speed: 750 rpm;

Initial pressure of oxygen: 1.0 MPa;

* In this experiment, alkali was KOH instead of NaOH.

References

1 M. Pagliaro, R. Ciriminna, H. Kimura, M. Rossi and C. Della Pina, *Angew. Chem. Int. Ed. Engl.*, 2007, 46, 4434-4440.

2 M. Pagliaro, M. Rossi, in The Future of Glycerol 2nd Edition, RSC Green Chemistry Book Series, **2010**.

3 B. Katryniok, S. Paul, F. Dumeignil, *ACS Catal.*, 2013, 3, 1819-1834.

4 B. Katryniok, H. Kimura, E. Skrzyńska, J.-S. Girardon, P. Fongarland, M. Capron, R. Ducoulombier, N. Mimura, S. Paul and F. Dumeignil, *Green Chem.*, 2011, 13, 1960-1979.

5 (a) H. Kimura, K. Tsuto, T. Wakisaka, Y. Kazumi and Y. Inaya, *Appl. Catal. A*, 1993, 96, 217-228, (b) H. Kimura, *Appl. Catal. A*, 1993, 105, 147-158.

6 M. Haruta, S. Tsubota, T. Kobayashi, H. Kageyama, M. J. Genet and B. Delmon, *J. Catal.*, 1993, 144, 175-192.

7 A. K. Sinha, S. Seelan, S. Tsubota and M. Haruta, *Angew. Chem. Int. Ed. Engl.*, 2004, 43, 1546-1548.

8 (a) S. Carrettin, P. McMorn, P. Johnston, K. Griffin and G. J. Hutchings, *Chem. Commun.*, 2002, 696-697, (b) S. Carrettin, P. McMorn, P. Johnston, K. Griffin, C. J. Kiely and G. J. Hutchings, *Phys. Chem. Chem. Phys.*, 2003, 5, 1329-1336, (c) N. Dimitratos, J. A. Lopez-Sanchez, J. M. Anthonykutty, G. Brett, A. F. Carley, R. C. Tiruvalam, A. A. Herzing, C. J. Kiely, D. W. Knight and G. J. Hutchings, *Phys. Chem. Chem. Phys.*, 2009, 11, 4952-4961.

9 (a) J. K. Edwards, B. E. Solsona, P. Landon, A. F. Carley, A. Herzing, C. J. Kiely and G. J. Hutchings, *J. Catal.*, 2005, 236, 69-79. (b) J. K. Edwards, B. Solsona, P. Landon, A. F. Carley, A. Herzing, M. Watanabe, C. J. Kiely and G. J. Hutchings, *J. Mater. Chem.*, 2005, 15, 4595-4600. (c) D. I. Enache, J. K. Edwards, P. Landon, B. Solsona-Espriu, A. F. Carley, A. A. Herzing, M. Watanabe, C. J. Kiely, D. W. Knight and G. J. Hutchings, *Science*, 2006, 311, 362-365. (There are too many references to list here all.)

10 (a) L. Kesavan, R. Tiruvalam, M. H. A. Rahim, M. I. bin Saiman, D. I. Enache, R. L. Jenkins, N. Dimitratos, J. A. Lopez-Sanchez, S. H. Taylor, D. W. Knight, C. J. Kiely and G. J. Hutchings, *Science*, 2011, 331, 195-199. (b) R. C. Tiruvalam, J. C. Pritchard, N. Dimitratos, J. A. Lopez-Sanchez, J. K. Edwards, A. F. Carley, G. J. Hutchings and C. J. Kiely, *Faraday Discuss.*, 2011, 152, 63-86. (c) A. Villa, D. Wang,

P. Spontoni, R. Arrigo, D. Su and L. Prati, *Catal. Today*, 2010, 157, 89-93. (d) A. Villa, N. Janjic, P. Spontoni, D. Wang, D. S. Su and L. Prati, *Applied Catalysis A: General*, 2009, 364, 221-228. (There are too many references to list here all.)

11 J. A. Lopez-Sanchez, N. Dimitratos, P. Miedziak, E. Ntainjua, J. K. Edwards, D. Morgan, A. F. Carley, R. Tiruvalam, C. J. Kiely and G. J. Hutchings, *Phys. Chem. Chem. Phys.*, 2008, 10, 1921-1930.

12 (a) C. L. Bianchi, P. Canton, N. Dimitratos, F. Porta and L. Prati, *Catal. Today*, 2005, 102-103, 203-212. (b) N. Dimitratos, J. Lopez-Sanchez, D. Lennon, F. Porta, L. Prati and A. Villa, *Catal. Lett.*, 2006, 108, 147-153. (c) N. Dimitratos, F. Porta and L. Prati, *Applied Catalysis A: General*, 2005, 291, 210-214. (d) N. Dimitratos, A. Villa and L. Prati, *Catal. Lett.*, 2009, 133, 334-340.

13 W. C. Ketchie, M. Murayama and R. J. Davis, *J. Catal.*, 2007, 250, 264-273.

14 G. L. Brett, Q. He, C. Hammond, P. J. Miedziak, N. Dimitratos, M. Sankar, A. A. Herzing, M. Conte, J. A. Lopez-Sanchez, C. J. Kiely, D. W. Knight, S. H. Taylor and G. J. Hutchings, *Angew. Chem. Int. Ed. Engl.*, 2011, 50, 10136-10139.

15 (a) T. Ishida, K. Kuroda, N. Kinoshita, W. Minagawa and M. Haruta, *J. Colloid Interface Sci.*, 2008, 323, 105-111, (b) T. Ishida, S. Okamoto, R. Makiyama and M. Haruta, *Appl. Catal. A*, 2009, 353, 243-248, (c) K. Kuroda, T. Ishida and M. Haruta, *J. Mol. Catal. A*, 2009, 298, 7-11, (d) T. Ishida and M. Haruta, *Angew. Chem. Int. Ed. Engl.*, 2007, 46, 7154-7156.

16 H. Miyamura, R. Matsubara, Y. Miyazaki and S. Kobayashi, *Angew. Chem. Int. Ed. Engl.*, 2007, 46, 4151-4154.

17 K. Mori, A. Hanafusa, M. Che and H. Yamashita, *J. Phys. Chem. Lett.*, 2010, 1, 1675-1678.

18 A. Villa, C. E. Chan-Thaw and L. Prati, *Appl. Catal. B*, 2010, 96, 541-547.

19 (a) R. W. J. Scott, O. M. Wilson, S.-K. Oh, E. A. Kenik and R. M. Crooks, *J. Am. Chem. Soc.*, 2004, 126, 15583-15591. (b) H.-L. Jiang, T. Akita, T. Ishida, M. Haruta and Q. Xu, *J. Am. Chem. Soc.*, 2011, 133, 1304-1306.

20 E. Skrzyńska, J. Ftouni, J.-S. Girardon, M. Capron, L. Jalowiecki-Duhamel, J.-F. Paul and F.Dumeignil. *Chem Sus Chem*, 2012, 5, 2065-2068.

21 Y. Ryabenkova, Q. He, P. J. Miedziak, N. F. Dummer, S. H. Taylor, A. F. Carley, D. J. Morgan, N. Dimitratos, D. J. Willock, D. Bethell, D. W. Knight, D. Chadwick, C. J. Kiely and G. J. Hutchings, *Catal. Today*, 2013, 203, 139-145.

Captions (figures and table)

Fig. 1 Setup of fixed bed flow reactor for oxidation of glycerol.

Fig. 2 Catalytic performances of Au-Pd nanoparticle catalysts with various Au atomic percentages.
○: Conversion of glycerol, ■: Summed selectivities to glyceric and tartronic acids (GLYA + TA.)
Reaction conditions:
Catalyst weight: 0.5 g (Content of (Au+Pd): 0.5 wt.%);
Glycerol concentration: 0.3 mol/L; Temperature: 333 K; Stirring speed: 750 rpm; Initial pressure of oxygen: 1.0 MPa.

Fig. 3 TEM image of Au-Pd nanoparticles stabilized in the ion-exchange resin.
(Catalyst No.1, Au+Pd = 0.5 wt.%, Au:Pd atomic ratio = 50:50.)

Fig. 4 STEM-HAADF image and size distribution of Au-Pd nano-particle in catalyst No.1.
(Statistics were performed on 78 particles. All STEM images for measuring size distribution are shown in Supporting information 1.)

Fig. 5 STEM-HAADF image and high-resolution EDS analysis of a typical Au-Pd nanoparticle observed in Catalyst No.1.

Fig. 6 STEM-HAADF image and size distribution of Au-Pd nano-particle in catalyst No.2.
(Statistics were performed on 89 particles. All STEM images for measuring size distribution are shown in Supporting information 1.)

Fig. 7 STEM-HAADF image and high-resolution EDS analysis of Au-Pd nano-particle in Catalyst No.2.

Fig. 8 STEM-HAADF image and size distribution of Au-Pd nano-particle in catalyst No.3.
(Statistics were performed on 93 particles. All STEM images for measuring size distribution are shown in Supporting information 1.)

Fig. 9 STEM-HAADF image and high-resolution EDS analysis of Au-Pd nano-particle in Catalyst No.3.

Fig. 10 Long-term catalytic reaction test of glycerol oxidation using flow type reactor.

0~1800 min: Glycerol solution liquid flow: 0.5 mL/min, Oxygen flow：3.5 mL/min
1800~4170 min: Glycerol solution liquid flow：0.6 mL/min, Oxygen flow：4.2 mL/min

Reactor: glass column for high pressure (inner diameter: 8.0 mm, length: 300 mm),
Catalyst weight: 5.0 g (volume: 8.3 mL), Reaction temperature: 333 K
Feed mixed solution liquid flow: glycerol 0.3 mol/L＋NaOH 1.2 mol/L
×: carbon balance, ◆: Conversion of glycerol, △: selectivity to glyceric acid, □: selectivity to tartronic acid.

Table 1 Effects of the preparation method and of the addition of NaOH on the catalytic performances of the Au:Pd 50:50 catalyst in the oxidation of glycerol using molecular oxygen as an oxidant.

Reaction conditions:
Catalyst weight: 0.5 g (Au/Pd atomic ratio: 1, content of (Au+Pd): 0.5 wt.%);
Glycerol concentration: 0.3 mol/L;
Temperature: 333 K;
Stirring speed: 750 rpm;
Initial pressure of oxygen: 1.0 MPa;
* In this experiment, alkali was KOH instead of NaOH.